https://doi.org/10.1016/j.apenergy.2021.117145

Performance characteristics of a liquid e-fuel cell

Xingyi Shi[#, 1], Xiaoyu Huo[#, 1], Oladapo Christopher Esan[1], Liang An*[, 1], T.S. Zhao*[, 2]

[1] Department of Mechanical Engineering, The Hong Kong Polytechnic University, Hung Hom, Kowloon, Hong Kong SAR, China

[2] Department of Mechanical and Aerospace Engineering, The Hong Kong University of Science and Technology, Clear Water Bay, Kowloon, Hong Kong SAR, China

[#] These authors contributed equally to this work.

* Corresponding authors.

Email: liang.an@polyu.edu.hk (L. An)

Email: metzhao@ust.hk (T.S. Zhao)

Abstract

Liquid fuel cell has been regarded as a promising power generation system due to its high energy density, instant recharging, and ease of fuel handling. However, its widespread commercialization is still being hampered by its limited performance resulting from the poor reaction kinetics of the conventional alcohol fuels. Recently, a liquid e-fuel cell, utilizing an electrically rechargeable liquid fuel (e-fuel), has been proposed and demonstrated with significant performance advancement in comparison to conventional liquid fuel cells. In this work, we study its performance characteristics and examine the effects of the operating and structural design parameters. Experimentally, it is found that this e-fuel cell, operating at 60˚C impressively results in an open-circuit voltage of 1.15 V, a maximum current density of 1980 mA cm^{-2}, a peak power density of 857.0 mW cm^{-2}, and an energy efficiency of 41.8 %. These significant results thus present that the liquid e-fuel cell opens a window of opportunity

for breakthroughs in advancement of fuel cell technology.

Keywords: E-fuel; Liquid e-fuel cells; Operating parameters; Structural design parameters; Power density; Energy efficiency

1. Introduction

In an attempt to reduce environmental pollutions and achieve sustainable energy development, more and more efforts have been devoted to develop alternative technologies for power generation in the last decades.[1] Fuel cells, as an advanced energy conversion system, which can continuously convert chemical energy into electricity, have therefore been extensively studied since its first invention in the middle of the 19th century.[2-4] After decades of research, hydrogen fuel cells, which utilize hydrogen as fuel with its fast reaction kinetics on the Pt catalysts and the zero-emission feature, are regarded as the most promising fuel cell system.[5-7] However, up till now, the real application of hydrogen fuel cells is still being constrained by some challenges mostly associated with the hydrogen production, storage and transportation. Therefore, liquid fuel cells, utilizing alcohol fuels towards achieving higher energy density and easier fuel handling, have been proposed and deeply investigated especially in recent years.[8, 9] Nonetheless, due to the sluggish reaction kinetics of alcohol liquid fuels, even on noble metal catalysts,[10, 11] the performances of conventional liquid fuel cells are still limited, which has greatly restricted their application scenarios. It is therefore of paramount importance to propose other potential fuels suitable for the operation of liquid fuel cells towards achieving a better performance.

Lately, an energy storage system utilizing an electrically rechargeable liquid fuel (e-fuel) as its energy storage medium has been proposed and studied.[12] This system possesses two major advantages: i) simultaneous and independent power generation (e-fuel cell) and energy storage (e-fuel charger); and ii) instantaneous rechargeability as

the exhausted e-fuel can be recycled and refilled into the cell. The utilized e-fuel can be made of various electroactive materials such as inorganic materials, organic materials, and suspension of particles. In addition, it possesses excellent reactivity even on carbon-based materials, which hence eliminates the usage of any noble metal electrocatalysts. Such feature thereby ensures low fabrication cost and superior durability of the system. Moreover, as the e-fuel is electrically rechargeable, it can further reduce the production and recycling cost of the fuel. In our previous study, the power generation potential of a liquid e-fuel cell at room temperature was successfully demonstrated, utilizing an e-fuel containing vanadium ions for anodic reaction paired with oxygen on the cathode side.[13] The liquid e-fuel cell, in more details, consists of a catalyst-free graphite-felt anode, a conventional oxygen cathode, and a proton exchange membrane. Even though the developed e-fuel cell has been proven to achieve a better performance in comparison to other common alcohol fuel cells operating at higher temperatures, its peak power density remains far below those of hydrogen fuel cells, and thus greatly hampered its real application in the future.[13] In this work, we study the performance characteristics of a liquid e-fuel cell and examine the effects of the operating and structural design parameters. It is experimentally found that this fabricated e-fuel cell achieved an extraordinarily high peak power density of 857.0 mW cm^{-2} and a maximum current density of 1980 mA cm^{-2} at 60 ˚C.

2. Working principle

The structure of the liquid e-fuel cell including a membrane electrode assembly (MEA), which is sequentially clamped by flow fields, heating plates, and current collectors is

shown in **Fig. 1.** It employs the oxygen reduction reaction (ORR) at its cathode side, while using a liquid e-fuel containing vanadium ions at its anode side. The overall reaction inside the cell is given as:

$$V^{2+} + \frac{1}{4}O_2 + H^+ \rightarrow V^{3+} + \frac{1}{2}H_2O \qquad E^0 = 1.49V \qquad (1)$$

By utilizing this liquid e-fuel, the cell achieves a high theoretical voltage of 1.49 V under standard state condition, which exceeds those of hydrogen fuel cells (1.23 V)[14] and other common alcohol fuel cells.

3. Experimental section

3.1 E-fuel cell

The MEA with an active area of 2.0 × 2.0 cm^2 was prepared using the previously reported method.[13] Four different kinds of cathode with various Pt/C catalyst loadings of 0.5, 1.0, 2.0 and 4.0 mg cm^{-2} were prepared. While four commercial membranes including Nafion 211 (25.4 μm), Nafion 212 (50.8 μm), Nafion 115 (127.0 μm) and Nafion 117 membranes (183.0 μm) with different thicknesses were pre-treated for further investigation. The graphite felt (AvCarb G100, Fuel Cell Store, USA) used as the anode was thermally treated in the air at 500˚C for 5 hours. The MEAs were assembled into the homemade fixture as previously reported to fabricate the liquid e-fuel cell.[13]

3.2 Experimental apparatus and test conditions

The experimental setup contains a liquid e-fuel cell, a proportional-integral-derivative (PID) temperature controller (Anthone Electronic Co. Ltd., China) and other relevant accessories. The PID temperature controller consists of a pair of heating rods and a pair of K-typed thermocouples for heating and temperature monitoring, respectively. During

the experiment, the cell was first heated while being fed with deionized water at anode and humidified oxygen with a flow rate of 250 sccm at cathode. When the cell reached the targeted operating temperatures, the deionized water was replaced by the e-fuel to conduct further tests. The e-fuel was first prepared by dissolving $VOSO_4$ powder into sulfuric acid and then charged using a flow cell.[13] The charged e-fuel was purged with nitrogen consistently during the whole experiment in order to prevent oxidation by the air. The polarization and constant-current discharging tests were conducted and recorded with a fuel cell testing system (Arbin BT2000, Arbin instrument Inc.). The electrochemical impedance spectroscopy (EIS) of the cell (from 0.01Hz to 100 kHz) was conducted by an electrochemical workstation (CHI-605C, CH Instruments, China). The X-ray diffraction (XRD) (Rint-2000, Rigaku, Japan) with Cu Kα radiation (λ = 0.15406 nm) and the scanning electron microscope (SEM) (SU5000, Hitachi, Japan) were used to examine the composition and morphology of the cathode, respectively, both before and after the long-term operation.

4. Results and discussion

4.1 General performance of this e-fuel cell

In this work, a liquid e-fuel cell assembled with the cathode of 4.0 mg cm^{-2} Pt working at 60 ˚C was examined. As shown in **Fig. 2 (a)**, the cell presents an open-circuit voltage of 1.15 V and demonstrates a peak power density of 857.0 mW cm^{-2}, which indicated that the performance was effectively enhanced. Such a superior peak power density not only substantially surpasses our previous work,[13] but also comparable to the hydrogen-oxygen fuel cells.[15-18] In addition, the cell further achieves an energy efficiency of 41.8 %

at 200 mA cm^{-2} (**Fig. 2 (b)**), demonstrating a much higher efficiency in comparison to the conventional alcohol fuel cells.[19-23] These results prove that increasing the operating temperature and the cathode catalyst loading are effective methods to overcome the major performance limitation of the liquid e-fuel cell resulting from the sluggish kinetics of the ORR.[24, 25] Thus, with the advantages of ease of e-fuel handling and fast response, this present cell is believed to be a promising competitor for real applications in the future.

4.2 Effect of the cathode catalyst loading

As mentioned, this liquid e-fuel cell, with the superior reactivity of liquid e-fuel even on graphite felt, successfully frees the anode from any catalysts.[13] On the other hand, the poor reactivity of oxygen at the cathode side becomes a great barrier hampering the overall cell performance. One common approach of improving the reactivity of oxygen is to increase the cathode catalyst loading, as a higher catalyst loading can provide a larger active surface area and thereby efficiently enhance the ORR.[26] Hence, to examine the influences of catalyst loading on the e-fuel cell performance, cathodes with four different Pt loadings of 0.5, 1.0, 2.0, and 4.0 mg cm^{-2} are prepared and assembled into the e-fuel cell for examination. A series of polarization curves and power density curves are obtained at room temperature (**Fig. 3 (a)**). It can be viewed that within the tested catalyst loading range, the e-fuel cell performance improves with the Pt loading. As the catalyst loading increases to 4.0 mg cm^{-2}, the maximum current density and peak power density boosts up to 1740.0 mA cm^{-2} and 588.7 mW cm^{-2}, respectively. Such an improved performance proves that the cathode catalyst loading is a crucial factor that

influences the reaction kinetics of oxygen reduction,[27] which further determines the overall cell performance. It is also worth to mention that, a further increase of the catalyst loading above 4.0 mg cm^{-2} is not examined in this study for two reasons. Firstly, a higher catalyst loading will induce a thicker catalyst layer, which may deteriorate the mass transport and also decline the ORR activity, thereby limiting the cell performance.[28] Moreover, to fulfill the requirement for real application, the capital cost of this system needs to be low. Considering the fact that the cell is able to generate a performance comparable to hydrogen fuel cells at 60 ˚C, with a loading of 4.0 mg cm^{-2}, a further increase of the catalyst loading is thus considered not to be cost-effective. Therefore, in this work, the cathode achieving the best performance with a Pt loading of 4.0 mg cm^{-2} is chosen for further studies.

4.3 Effect of the membrane thickness

Membrane is one of the most crucial components in the liquid e-fuel cell. On one hand, it plays an important role to prevent the crossover of liquid e-fuel, as the permeation of e-fuel to the cathode would lead to mixed potential and further results in large voltage loss.[29, 30] On the other hand, it should also allow the ease of protons transport between the two half-cells so as to reduce ohmic loss. As widely demonstrated before, the commercial Nafion membranes with a large thickness could prevent the crossover of reactive species more effectively, while it may also lead to higher internal resistance, which thereby results in significant voltage loss according to the Ohm's law.[31, 32] Hence, to examine the effect of membrane thickness, membranes including Nafion 117 (183.0 μm), Nafion 115 (127.0 μm), Nafion 212 (50.8 μm) and Nafion 211 (25.4 μm) are

selected for investigation at room temperature (**Fig. 3 (b)**). It can be viewed from the polarization curves that, as the membrane thickness increases, the liquid e-fuel cell performance decreases. Overall, the cell assembled with the membrane of the least thickness (25.4 μm) outperforms the other membranes, demonstrating the best performance. Such result suggests that the ohmic resistance of the membrane plays a key role on the cell performance, while the influences of crossover seems not to be obvious. However, it is predicted that a thin membrane may eventually induce severe crossover of reactive species, thereby limiting the cell performance. Hence, in this work, to ensure the cell with a higher peak power density, Nafion 211 membrane is considered as the best choice for the liquid e-fuel cell.

4.4 Effect of the operating temperature

As mentioned in the previous section, the sluggish kinetics at cathode is one of the major limitations restraining the overall e-fuel cell performance. To overcome this problem, other than increasing the cathode catalyst loading, raising the operating temperature is another effective approach that has been widely demonstrated.[33, 34] Hence, to examine the effect of the operating temperature, experiments were conducted from 23 to 60˚C as shown in **Fig. 3 (c)**. It is found that, when operated at 60˚C, the cell achieves a maximum current density of 1980.0 mA cm^{-2} with a peak power density of 857.0 mW cm^{-2}, which thus significantly exceeds our previous work with a peak power density of 293 mW cm^{-2}.[13] Its performance improvement under a higher operating temperature can be mainly attributed to the following reasons. Firstly, the elevation of operating temperature is an effective method that improves the sluggish reaction kinetic

of oxygen reduction,[35] and thereby reduces the voltage loss. Furthermore, while the e-fuel is able to exhibit fast reaction kinetic even under room temperature due to its good reactivity, the higher operating temperature can indeed improves the e-fuel conductivity and lowers the viscosity,[36] which facilitates the reactants transport and thereby reduces the cell internal resistance.[26, 37, 38] Additionally, the ionic conductivity of Nafion 211 membrane is also closely related to the operating temperature, and a higher ionic conductivity can be presented at 60˚C due to the improved diffusion and migration process of protons through the membrane.[39-41] In summary, with the increase of the operating temperature, the resistance of e-fuel cell can be reduced as proven by the EIS results (**Fig. 3 (d)**), which in turn leads to the exceptionally high cell performance. However, it is worth to mention that, the elevated operating temperature would, on the other hand, result in a more aggravated cross-over of vanadium ions and oxygen molecules through the membrane,[42] which would eventually lead to a severe fuel loss and performance degradation of the system.

4.5 Constant-current discharging behavior

The constant-current discharging test is widely applied for the examination of the actual operating behavior as well as the energy losses of a fuel cell system. Utilizing this method, here, the e-fuel cell was tested under an operating temperature range from 23 to 60˚C at 200 mA cm^{-2} with the e-fuel containing 0.75 M V(II), as shown in **Fig. 4 (a)**. The associated energy losses (**Figs. S1-4**) and three efficiencies are also calculated and summarized in **Fig. 4 (b)**. It is observed that the increase of operating temperature leads to an increased discharge voltage plateau and thereby a higher voltage efficiency (VE),

which primarily results from the lowered cell resistance in view of the enhanced conductivities of both the liquid e-fuel and the membrane as demonstrated earlier in **Fig. 3 (d)**.[36, 43] Furthermore, this temperature variation also results in a higher discharge capacity, which is due to the fact that the elevated temperature can accelerate the reaction kinetics on both sides, enhancing the utilization of the liquid e-fuel. However, it is worth mentioning that, as the temperature rises, it simultaneously leads to an aggravated crossover of both the e-fuel and oxygen molecules,[37, 44] which would result into a serious capacity loss. Overall, only a minor improvement on the discharge capacity are found. Nonetheless, the energy efficiency (EE) of the e-fuel cell elevates from 36.6% to 41.8% with the temperature increase to 60˚C, proving that high operating temperature can effectively improve the discharging performance of this liquid e-fuel cell.

4.6 Long-term discharging behavior

Long-term stability is of significant importance before realizing the widespread application of a fuel cell system.[45] Here, to examine the ability of this cell for long-term operation, the cell has been refueled for 50 times and discharged at 10 mA cm^{-2} at 60˚C. The discharge curves are presented in **Fig. 5 (a)**, while the efficiencies of these 50 cycles are calculated in **Fig. 5 (b)**. It is shown that the present system is able to achieve a continuous and stable power generation for nearly 60 hours, with its almost instantaneous rechargeability through replacing the exhausted e-fuel with fresh ones. Furthermore, the cell also presents a relatively stable efficiency, with only a minor EE decrease of 1.4 % after 50 times refueling, indicating its potential for stable operation

at high operating temperatures. However, it is noteworthy that the EE of this system at 10 mA cm^{-2} is much lower in comparison to its efficiency achieved at 200 mA cm^{-2} (**Fig. 4 (b)**), which is attributed to the prolonged discharge duration leading to a more serious crossover of reactive species and a lower e-fuel utilization efficiency.[46, 47] Hence, in the future, the development of a membrane with better selectivity could be a research direction with great importance for the enhancement of the liquid e-fuel cell performance of long-term operation at higher operating current densities. After the long-term operation test, the cell was then disassembled and the MEA without any obvious appearance damage can be seen as shown in **Fig. S5**. To further examine the durability of the cathode, its XRD patterns (**Fig. 5 (c)**) and SEM images (**Fig. 5 (d)**), both before and after the long-term operation are obtained. It can be seen from these results that, little changes can be observed after the long-term operation, indicating the good chemical stability of the cathode, which again proves the capability of this liquid e-fuel cell for long-term operation.

5. Summary

In this work, we have demonstrated the operation of an e-fuel cell that is free of anode catalysts and capable of achieving a peak power density of 857.0 mW cm^{-2} at 60˚C. It is revealed that a higher catalyst loading at the cathode side, along with the increase of operating temperature, can effectively resolve the limitation induced from the sluggish ORR kinetic and further boost the cell performance. In addition, the cell further attains an energy efficiency of 41.8 % even at 200 mA cm^{-2} with a stable operation of ~60 hours, illustrating its ability for efficient power generation and excellent long-term

operation stability. It should be mentioned that the increase of operating temperature and the decrease of membrane thickness present a positive effect on the cell performance, but both can induce severe crossover of reactive species thereby deteriorating the cell performance especially during constant-current discharging. Hence, with the development of membranes with better selectivity and catalysts with better catalytic reactivity for oxygen reduction reaction, it is believed that this e-fuel cell could achieve even better performance, positioning it as a promising power generation technology in the future.

Acknowledgement

The work described in this paper was fully supported by a grant from the Research Grant Council of the Hong Kong Special Administrative Region, China (Project No. T23-601/17-R).

References

1. M. Contestabile, G. Offer, R. Slade, F. Jaeger and M. Thoennes, *Energy & Environmental Science*, 2011, **4**, 3754-3772.
2. K.-S. Lee, J. S. Spendelow, Y.-K. Choe, C. Fujimoto and Y. S. Kim, *Nature energy*, 2016, **1**, 16120.
3. D. Y. Chung, J. M. Yoo and Y. E. Sung, *Advanced Materials*, 2018, **30**, 1704123.
4. X. Yuan, X.-L. Ding, C.-Y. Wang and Z.-F. Ma, *Energy & Environmental Science*, 2013, **6**, 1105-1124.
5. M. Lopez-Haro, L. Guétaz, T. Printemps, A. Morin, S. Escribano, P.-H. Jouneau, P. Bayle-Guillemaud, F. Chandezon and G. Gebel, *Nature communications*, 2014, **5**, 1-6.
6. Y.-C. Chiang and J.-R. Ciou, *International Journal of Hydrogen Energy*, 2011, **36**, 6826-6831.
7. J. Zhang, Z. Xie, J. Zhang, Y. Tang, C. Song, T. Navessin, Z. Shi, D. Song, H. Wang and D. P. Wilkinson, *Journal of Power Sources*, 2006, **160**, 872-891.
8. W. Huang, H. Wang, J. Zhou, J. Wang, P. N. Duchesne, D. Muir, P. Zhang, N. Han, F. Zhao and M. Zeng, *Nature communications*, 2015, **6**, 1-8.
9. S. Han, Y. Yun, K. W. Park, Y. E. Sung and T. Hyeon, *Advanced Materials*, 2003, **15**, 1922-1925.
10. S. Song and P. Tsiakaras, *Applied Catalysis B: Environmental*, 2006, **63**, 187-193.
11. C. Liu, W. Zhou, J. Zhang, Z. Chen, S. Liu, Y. Zhang, J. Yang, L. Xu, W. Hu and Y. Chen, *Advanced Energy Materials*, 2020, **10**, 2001397.
12. H. Jiang, L. Wei, X. Fan, J. Xu, W. Shyy and T. Zhao, *Science Bulletin*, 2019, **64**, 270-280.
13. X. Shi, X. Huo, Y. Ma, Z. Pan and L. An, *Cell Reports Physical Science*, 2020, **1**, 100102.
14. S. A. M. Shaegh, N.-T. Nguyen, S. M. M. Ehteshami and S. H. Chan, *Energy & Environmental Science*, 2012, **5**, 8225-8228.
15. J. Liu, M. Jiao, L. Lu, H. M. Barkholtz, Y. Li, Y. Wang, L. Jiang, Z. Wu, D.-j. Liu and L. Zhuang, *Nature communications*, 2017, **8**, 1-10.
16. N. Steffy, V. Parthiban and A. Sahu, *Journal of Membrane Science*, 2018, **563**, 65-74.
17. H.-F. Lee, J.-Y. Chang and Y. W. Chen-Yang, *RSC advances*, 2018, **8**, 22506-22514.
18. V. M. Umap and R. P. Ugwekar, *Renewable Energy*, 2020.
19. H. Deng, Y. Zhang, X. Zheng, Y. Li, X. Zhang and X. Liu, *Energy*, 2015, **82**, 236-241.
20. F. Zhang, J. Jiang, Y. Zhou, J. Xu, Q. Huang, Z. Zou, J. Fang and H. Yang, *Fuel Cells*, 2017, **17**, 315-320.
21. Z. Yuan, W. Chuai, Z. Guo, Z. Tu and F. Kong, *Energy Storage*, 2019, **1**, e64.
22. V. Bambagioni, C. Bianchini, Y. Chen, J. Filippi, P. Fornasiero, M. Innocenti, A. Lavacchi, A. Marchionni, W. Oberhauser and F. Vizza, *ChemSusChem*, 2012, **5**,

1266-1273.
23. L. Wang, A. Lavacchi, M. Bevilacqua, M. Bellini, P. Fornasiero, J. Filippi, M. Innocenti, A. Marchionni, H. A. Miller and F. Vizza, *ChemCatChem*, 2015, **7**, 2214-2221.
24. Y. Chen, S. Ji, S. Zhao, W. Chen, J. Dong, W.-C. Cheong, R. Shen, X. Wen, L. Zheng and A. I. Rykov, *Nature communications*, 2018, **9**, 1-12.
25. H. S. Casalongue, S. Kaya, V. Viswanathan, D. J. Miller, D. Friebel, H. A. Hansen, J. K. Nørskov, A. Nilsson and H. Ogasawara, *Nature communications*, 2013, **4**, 1-6.
26. T. Kadioglu, A. C. Turkmen, K. C. Ata, R. G. Akay, I. Tikiz and C. Celik, *International Journal of Hydrogen Energy*, 2020, **45**, 35006-35012.
27. H. Gasteiger and S. Yan, *Journal of power sources*, 2004, **127**, 162-171.
28. Y.-H. Shih, G. V. Sagar and S. D. Lin, *The Journal of Physical Chemistry C*, 2008, **112**, 123-130.
29. S. Jeong, L.-H. Kim, Y. Kwon and S. Kim, *Korean Journal of Chemical Engineering*, 2014, **31**, 2081-2087.
30. X. Shi, O. C. Esan, X. Huo, Y. Ma, Z. Pan, L. An and T. Zhao, *Progress in Energy and Combustion Science*, 2021, **85**, 100926.
31. B. Jiang, L. Wu, L. Yu, X. Qiu and J. Xi, *Journal of Membrane Science*, 2016, **510**, 18-26.
32. D. Chen, M. A. Hickner, E. Agar and E. C. Kumbur, *Journal of Membrane Science*, 2013, **437**, 108-113.
33. A. Chandan, M. Hattenberger, A. El-Kharouf, S. Du, A. Dhir, V. Self, B. G. Pollet, A. Ingram and W. Bujalski, *Journal of Power Sources*, 2013, **231**, 264-278.
34. Q. Wu, L. An, X. Yan and T. Zhao, *Electrochimica Acta*, 2014, **133**, 8-15.
35. H. Xu, Y. Song, H. R. Kunz and J. M. Fenton, *Journal of the Electrochemical Society*, 2005, **152**, A1828.
36. S. Xiao, L. Yu, L. Wu, L. Liu, X. Qiu and J. Xi, *Electrochimica Acta*, 2016, **187**, 525-534.
37. J. Xi, S. Xiao, L. Yu, L. Wu, L. Liu and X. Qiu, *Electrochimica Acta*, 2016, **191**, 695-704.
38. L. An, T. Zhao, S. Shen, Q. Wu and R. Chen, *Journal of Power Sources*, 2011, **196**, 186-190.
39. P. Dimitrova, K. Friedrich, B. Vogt and U. Stimming, *Journal of Electroanalytical Chemistry*, 2002, **532**, 75-83.
40. G. G. Kumar, A. Kim, K. S. Nahm and R. Elizabeth, *International Journal of Hydrogen Energy*, 2009, **34**, 9788-9794.
41. J. Peron, A. Mani, X. Zhao, D. Edwards, M. Adachi, T. Soboleva, Z. Shi, Z. Xie, T. Navessin and S. Holdcroft, *Journal of Membrane Science*, 2010, **356**, 44-51.
42. R. Badrinarayanan, J. Zhao, K. Tseng and M. Skyllas-Kazacos, *Journal of Power Sources*, 2014, **270**, 576-586.
43. Y. Cheng, H. Zhang, Q. Lai, X. Li, Q. Zheng, X. Xi and C. Ding, *Journal of Power Sources*, 2014, **249**, 435-439.

44. S. Ma and E. Skou, *Solid State Ionics*, 2007, **178**, 615-619.
45. M. S. Masdar, A. M. Zainoodin, M. I. Rosli, S. K. Kamarudin and W. R. W. Daud, *International Journal of Hydrogen Energy*, 2017, **42**, 9230-9242.
46. X. Zhou, T. Zhao, L. An, L. Wei and C. Zhang, *Electrochimica Acta*, 2015, **153**, 492-498.
47. Y.-J. Chiu, *International Journal of Hydrogen Energy*, 2010, **35**, 6418-6430.

Figure captions

Figure 1 Working principle of an e-fuel cell.

Figure 2 (a-b) General performance of this liquid e-fuel cell at 60˚C.

Figure 3 (a-b) Polarization curves and power density curves of this liquid e-fuel cell with various cathode catalyst loadings and membrane thicknesses and (c-d) polarization, power density, and EIS curves at various operating temperatures.

Figure 4. (a) Constant-current discharging behaviors and (b) comparison of three efficiencies at various operating temperatures.

Figure 5 (a-b) Long-term discharging behaviors and the comparison of 1^{st} and 50^{th} discharging curves (insert); (c-d) XRD curves and SEM images of the cathode catalyst layer (i) before and (ii) after long-term discharging.

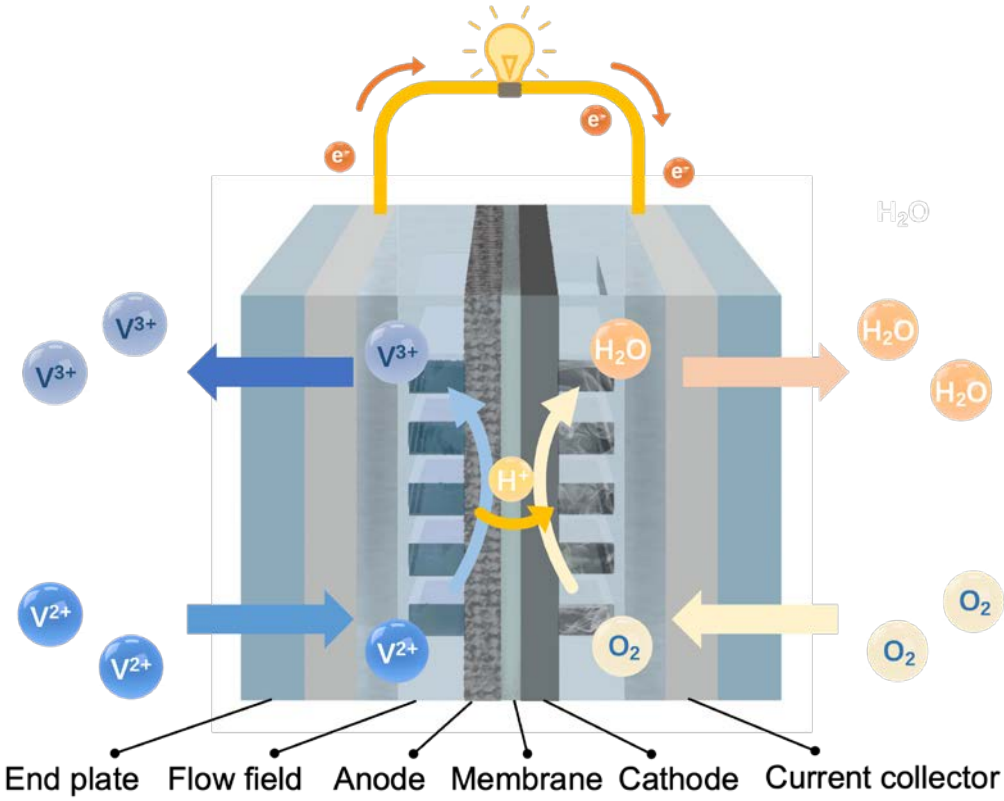

Figure 1 Working principle of an e-fuel cell.

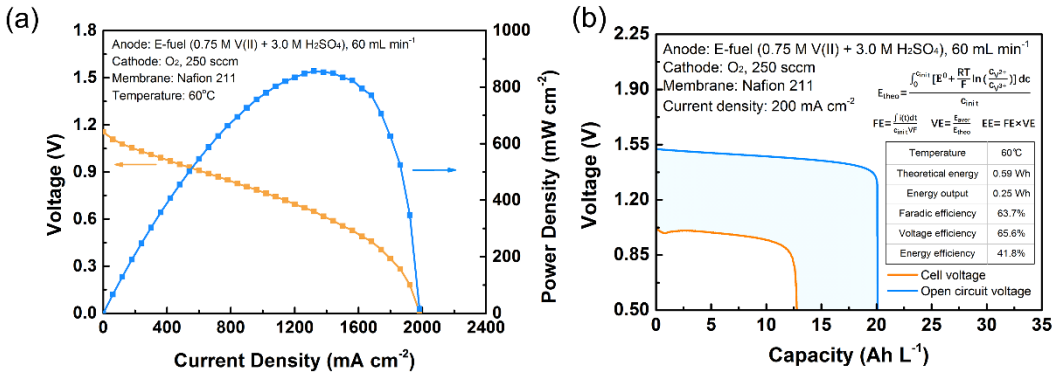

Figure 2 (a-b) General performance of this liquid e-fuel cell at 60˚C.

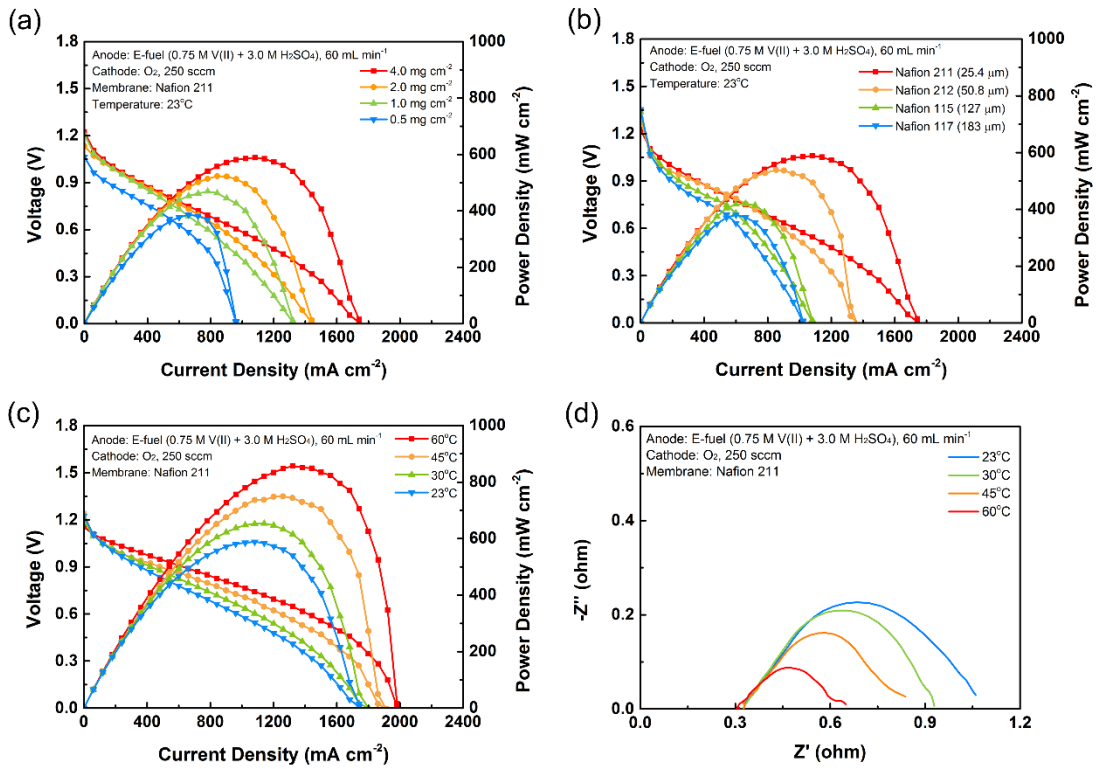

Figure 3 (a-b) Polarization curves and power density curves of this liquid e-fuel cell with various cathode catalyst loadings and membrane thicknesses and (c-d) polarization, power density, and EIS curves at various operating temperatures.

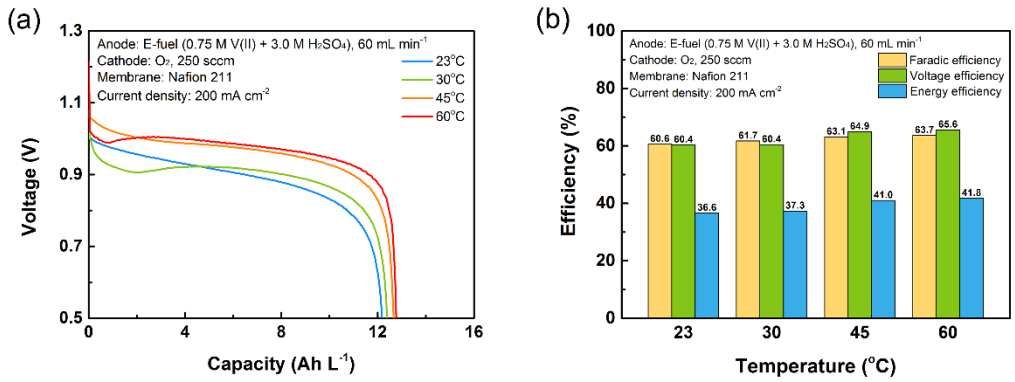

Figure 4 (a) Constant-current discharging behaviors and (b) comparison of three efficiencies at various operating temperatures.

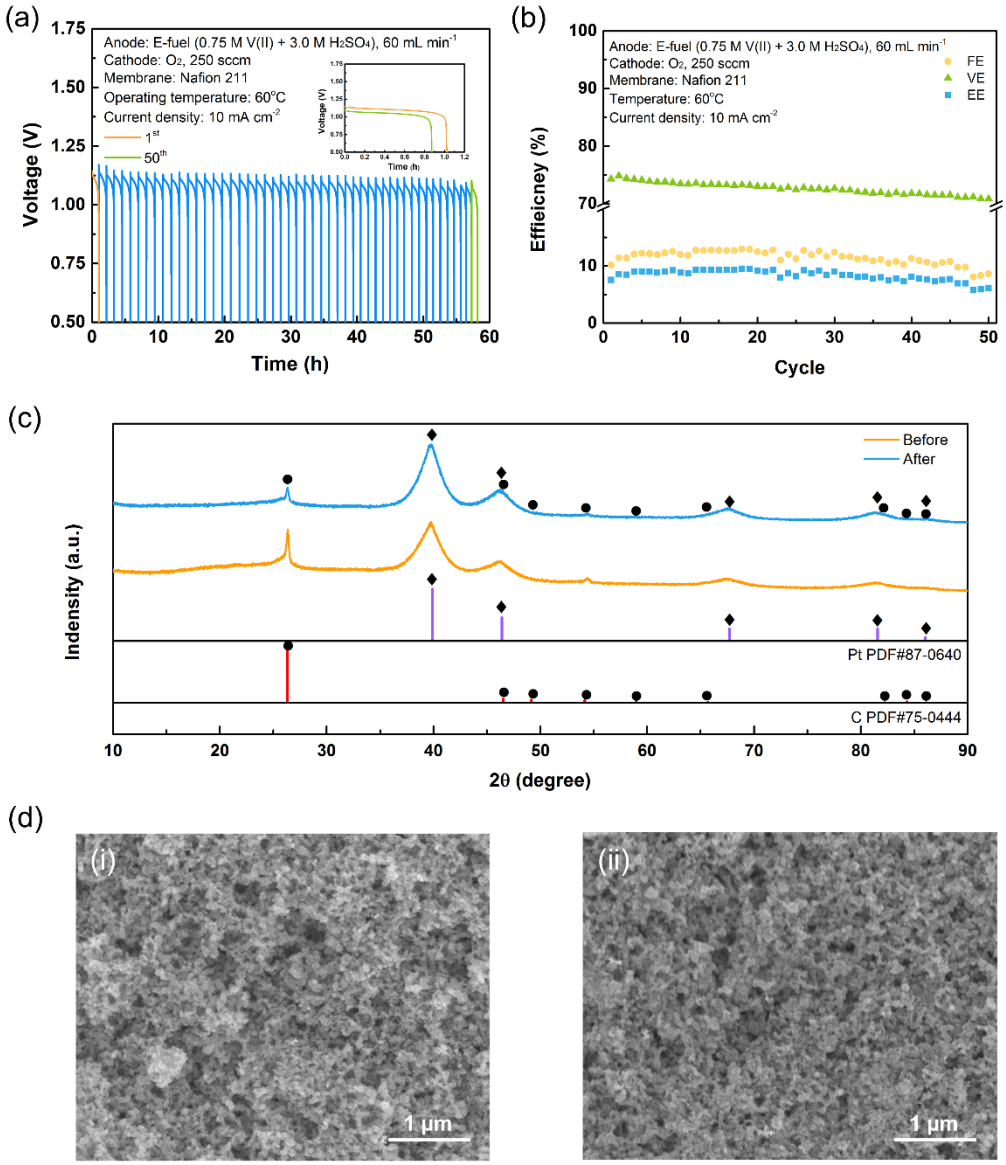

Figure 5 (a-b) Long-term discharging behaviors and the comparison of 1st and 50th discharging curves (insert); (c-d) XRD curves and SEM images of the cathode catalyst layer (i) before and (ii) after long-term discharging.